

Luminescence efficiency of europium-doped LGS, LGT and LGN crystals

S. GEORGESCU*, A. M. VOICULESCU, O. TOMA, L. GHEORGHE, A. ACHIM, C. MATEI, S. HAU
National Institute for Laser, Plasma and Radiation Physics, Magurele, Romania

In order to evaluate the possibilities of Eu-doped langasite, langanite, and langatate as red phosphors, we estimate the quantum efficiency of 5D_0 level and the relative quantum yield. The radiative lifetime is obtained from the luminescence spectra calibrated with the magnetic dipole transition ${}^5D_0 \rightarrow {}^7F_1$. The comparison of the radiative lifetimes and the measured lifetimes allows the calculation of the quantum efficiency of 5D_0 level. The diffuse reflectance spectra are used to compare the relative quantum yields of these materials with the quantum yield of a more efficient phosphor, Eu-doped YVO₄, previously synthesized by us. The quantum yield of Eu-doped langasite, langanite, and langatate represents approximately 60% of the quantum yield of our Eu:YVO₄.

(Received November 8, 2010; accepted November 29, 2010)

Keywords: Langasite, Langanite, Langatate, Eu³⁺, Quantum efficiency, Quantum yield

1. Introduction

LGX crystals, i.e. langasite (La₃Ga₅SiO₁₄ - LGS), langanite (La₃Ga_{5.5}Nb_{0.5}O₁₄ - LGN) and langatate (La₃Ga_{5.5}Ta_{0.5}O₁₄ - LGT), crystallise in the *P321* space group, symmetry class *32* and are isostructural with the calciumgallogermanate (Ca₃Ga₂Ge₄O₁₄) [1, 2]. The general formula is *A*₃*BC*₃*D*₂O₁₄ where *A* represents the dodecahedral positions (distorted Thompson cubes), *B* – octahedral positions and *C*, *D* – tetrahedral positions. La³⁺ occupies the position *A*. The local symmetry at this site is C₂ [3]. In contrast with LGS where Ga³⁺ and Si⁴⁺ share with equal probability the tetrahedral positions *D*, in LGN (LGT) the octahedral positions *B* are occupied by two different ions, Ga³⁺ and Nb³⁺ (Ta⁵⁺) (also, with equal probability). Ga³⁺ occupies the remaining positions (*C* and *D*). The structural difference between LGS and LGN (or LGT) consists in the placement of the shortest distance positions randomly occupied around the *A* site: four positions in the plane perpendicular on the C₂ axis for LGS and two positions along the C₂ axis in LGN and LGT. Besides, there is a larger charge difference between Nb⁵⁺ (or Ta⁵⁺) and Ga³⁺ than between Si⁴⁺ and Ga³⁺ [4, 5].

When excited in the near UV (396 nm, transition ${}^7F_0 \rightarrow {}^5L_6$), Eu³⁺-doped LGS, LGT, and LGN crystals show bright red luminescence which suggests the possibility to use these materials as red phosphors. Besides, the disorder of these crystals results in wider absorption bands of Eu³⁺, improving the matching between the absorption lines and the spectrum of the light-emitting diodes. An analysis of the luminescence of Eu³⁺ in LGS and LGT crystals was presented in [4, 5]. It was shown that the Eu³⁺ - O²⁻ bond is more covalent in LGT while the crystal field at the Eu³⁺ is stronger in LGS.

In this paper, we calculate the quantum efficiency of the 5D_0 level (the ratio between the measured and the radiative lifetime) in europium-doped LGS, LGN and LGT crystals, the radiative lifetime being obtained from the

luminescence spectra, using the magnetic-dipole transition ${}^5D_0 \rightarrow {}^7F_1$ as an internal standard. Since the diffuse reflectance spectra of Eu-doped LGS, LGN, and LGT crystal powders, measured with the experimental setup presented in [6], shows simultaneously both absorption and emission (transition ${}^5D_0 \rightarrow {}^7F_2$) lines, we calculate the relative quantum yield based on the areas of the emission and absorption Eu³⁺ lines. For a preliminary characterisation of the phosphor qualities of Eu:LGX, the diffuse reflectance spectra are used to compare the quantum yield of the Eu:LGX crystals with the quantum yield of a more efficient red phosphor, Eu-doped YVO₄, synthesized previously by us [7].

2. Experimental

Eu-doped LGX (LGS, LGN and LGT) crystals were synthesized in our laboratory from high-purity La₂O₃, Ga₂O₃, SiO₂, Nb₂O₅, Ta₂O₅, and Eu₂O₃, according to (La_{0.95}Eu_{0.05})₃Ga₅SiO₄, (La_{0.97}Eu_{0.03})₃Ga_{5.5}Nb_{0.5}O₁₄, and (La_{0.97}Eu_{0.03})₃Ga_{5.5}Ta_{0.5}O₁₄ formulae. The oxides were mixed in an agate balls mill and calcinated at 1500 °C for 24 h. The powder was pressed in pallets and the crystals were grown along the C axis in platinum crucibles in nitrogen atmosphere, using the Czochralski method. The powder of Eu³⁺-doped LGN was obtained by milling of single crystals.

The luminescence of the Eu:LGN was excited using a ScienceTech Xe-Hg 350-W lamp with suitable filters. The fluorescence spectra were measured at room temperature using a Horiba Jobin-Yvon 1000M monochromator, an S-20 photomultiplier and a SR830 lock-in amplifier from Stanford Research Systems. For decay measurements, the luminescence was excited with the second harmonic of a Nd-YAG laser and analyzed with an Ortec MCS-PCI multichannel scaler card. All measurements were performed at room temperature.

3. Results and discussion

In Fig. 1 are given the luminescence spectra of Eu^{3+} in LGS, LGN, and LGT powders containing the lines corresponding to the ${}^5D_0 \rightarrow {}^7F_J$ ($J = 0, 1, \dots, 4$) transitions. The remaining transitions (for $J = 5, 6$) were neglected due to their very low intensities. Possible superposition with lines from higher Eu^{3+} levels (${}^5D_1, {}^5D_2, {}^5D_3$) is eliminated adjusting the phase of the lock-in amplifier. This elimination is possible due to the large difference between the lifetime of 5D_0 (~ 1 ms) and lifetimes of the higher levels (tens of microseconds), as obtained from the decay measurements. The choice of powder instead of single crystals is justified by: (i) we are interested to evaluate the possibilities of Eu-doped LGN as a red phosphor which is usually a powder, (ii) the anisotropy of the LGN crystals is eliminated; (iii) an easier comparison with Eu-LGN synthesized by other methods (e. g., sol-gel).

The luminescence spectrum of Eu^{3+} allows a simple determination of the radiative lifetimes. The magnetic-dipole transition (${}^5D_0 \rightarrow {}^7F_1$) is practically insensitive to the changes in the neighborhood of Eu^{3+} ion and is used as an internal standard [8, 9]. Its probability can be calculated using the expressions given in [8, 10], provided that the free-ion eigenfunctions are known. The value of its probability in vacuum is $A_0^{md} = 14.65 \text{ s}^{-1}$ [11]. In a medium with the refraction index n

$$A^{md} = n^3 A_0^{md} \quad (1)$$

The refraction indexes for LGS, LGN, and LGT crystals are given in [12]. For the powder, the values of n were averaged on the orientations: $n = (2n_o + n_e)/3$, where n_o and n_e represent the ordinary, respectively extraordinary refraction indices. The n values for ${}^5D_0 \rightarrow {}^7F_1$ transition for LGS, LGN, and LGT crystals together with the probability of the magnetic dipole transitions are given in Table 1.

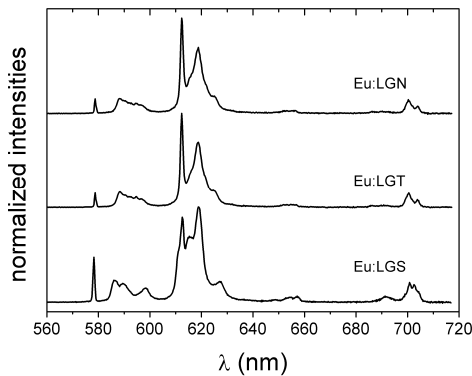


Fig. 1. Luminescence spectra of Eu-doped LGN, LGT, and LGS. The spectra are corrected for the sensitivity of the experimental apparatus; the luminescence lines from higher 5D_J levels was eliminated by a proper choice of the lockin phase.

The radiative lifetime of the 5D_0 level can be obtained from the luminescence spectrum corrected for the spectral sensitivity of the experimental setup [11].

$$\frac{1}{\tau_{rad}({}^5D_0)} = A^{md}({}^5D_0 \rightarrow {}^7F_1) \frac{I_{tot}}{I({}^5D_0 \rightarrow {}^7F_1)} \quad (2)$$

where $I_{tot}/I({}^5D_0 \rightarrow {}^7F_1)$ is the ratio of the total area of the luminescence spectrum (Fig. 1) and the area of the magnetic-dipole transition. The results are given in Table 1.

The quantum efficiency of the luminescent level is given by

$$\eta = \tau_{fl} / \tau_{rad} \quad (3)$$

where τ_{fl} is the measured lifetime. The decay curve of the 5D_0 level for pumping in 5D_1 (pump transition ${}^7F_1 \rightarrow {}^5D_1$) for Eu:LGN is given in Fig. 2. The kinetics of 5D_0 level of Eu^{3+} in LGS and LGT crystals was measured in [4]. For all Eu:LGX crystals examined in this paper the decay of 5D_0 is very close to exponential. The observed risetime is due to the kinetics of 5D_1 level. Its values are, respectively, 26 μs and 62 μs for LGS and LGT [4] and 67 μs for LGN. The values of τ_{fl} and η_{eff} are also given in Table 1.

The subunitary values of the quantum efficiency of 5D_0 level for the Eu:LGX crystals cannot be explained by multiphonon processes. For a gap (between 5D_0 and 7F_6) of $\sim 12000 \text{ cm}^{-1}$, only OH^- impurities can have noticeable effects. Since LGX powders were not obtained by wet methods, OH^- , as an efficient quencher can be excluded. More probably, the subunitary values of the quantum efficiency could be related to transfer to random impurities.

Table 1. The refractive index (n), the probability of the magnetic dipole transition ${}^5D_0 \rightarrow {}^7F_1$ (A^{md}), radiative (τ_{rad}) and fluorescence (τ_{fl}) lifetimes, and quantum efficiency (η_{eff}) of 5D_0 level of Eu^{3+} in LGS, LGN, and LGT crystals.

Crystal	LGS	LGN	LGT
n	1.910	1.969	1.953
$A^{md} (\text{s}^{-1})$	102	112	109
$\tau_{rad} (\mu\text{s})$	1600	1400	1450
$\tau_{fl} (\mu\text{s})$	1010 ^{a)}	1046 ^{b)}	1035 ^{a)}
η_{eff}	0.63	0.75	0.71

^{a)}from Ref. 4; ^{b)}this paper.

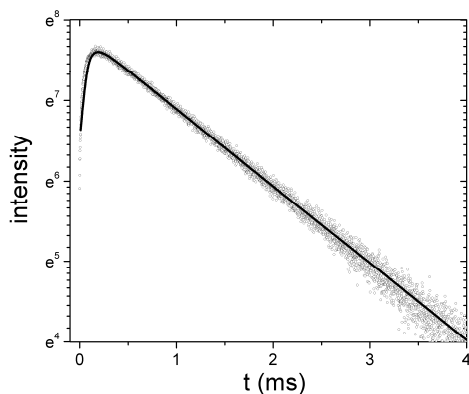


Fig. 2. Kinetics of the 5D_0 level in Eu:LGN crystal for pumping in 5D_1 .

Since the ${}^5D_0 \rightarrow {}^7F_2$ transition is, by far, the most intense (see Fig. 1), the difference between the radiative lifetimes of Eu-doped LGS, LGT and LGN crystals is given, mainly, by the ratio $R_{20} = I({}^5D_0 \rightarrow {}^7F_2) / I({}^5D_0 \rightarrow {}^7F_1)$. In Ref. [4] we found that the value of $R_{20}(\text{LGT}) > R_{20}(\text{LGS})$ explained by a higher covalency for LGT, in agreement with the increase of the red shift of ${}^5D_0 \rightarrow {}^7F_0$ line from LGS to LGT. Because the structure of the LGN crystals is very close to the LGT structure, we expect the same red shift of ${}^5D_0 \rightarrow {}^7F_0$ in LGT and LGN. This is illustrated in Fig. 3. This explains the close values of the radiative lifetime of 5D_0 in LGT and LGN. On the other hand, a lower value of R_{20} (lower covalency) for LGS increases the value of the radiative lifetime.

The diffuse reflectance spectra measured on europium-doped LGS, LGN, and LGT powders are given in Fig. 4.

The baselines of the diffuse reflectance spectra of Eu-doped LGS, LGN, and LGT crystal powders [6], tilted toward short wavelengths region, reflect the reddish coloration produced by the point defects involving oxygen [13-16].

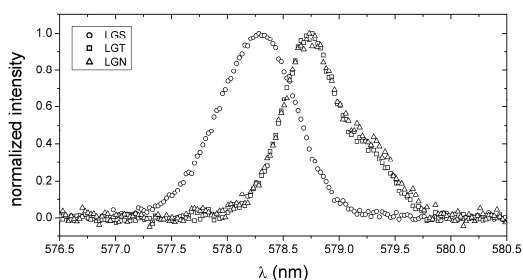


Fig. 3. ${}^5D_0 \rightarrow {}^7F_0$ transition in Eu-doped LGX crystals.

For comparison, in the same figure, is shown the diffuse reflectance spectrum of a Eu-doped YVO_4 powder annealed in air at 800 °C, synthesized in our laboratory [17]. In the absence of a commercial Eu: YVO_4 powder with known efficiency, we have chosen our Eu: YVO_4 powder annealed at 800 °C, which proved the highest

efficiency. The baseline of its reflectance spectrum is, also, tilted toward short wavelengths (the origin of the yellowish color of YVO_4 was discussed in [18-20]).

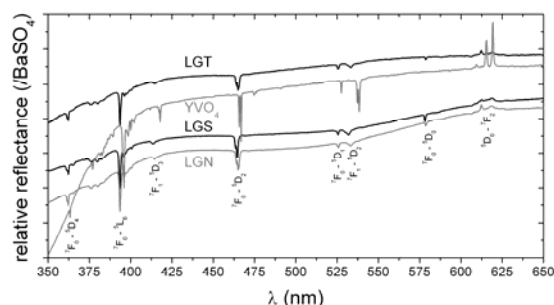


Fig. 4. Diffuse reflectance spectra (in rapport with BaSO_4) of Eu-doped LGS, LGN, and LGT crystal powders. For comparison, the reflectance spectrum of the Eu-doped YVO_4 powder is shown. The reflectance curves are shifted on the vertical scale for a better visualization.

The Eu^{3+} $f-f$ transitions appear as narrow features in the diffuse reflectance spectra. Besides the ${}^7F_1 \leftrightarrow {}^5D_0$ and ${}^7F_2 \leftrightarrow {}^5D_0$, the $f-f$ transitions appear as absorption lines. ${}^7F_2 \leftrightarrow {}^5D_0$ is seen as luminescent while ${}^7F_1 \leftrightarrow {}^5D_0$ is practically absent (for Eu-doped LGX powders as well as for Eu: YVO_4). A qualitative explanation of this situation can be done, based on the energy level schema and the peculiar excitation source (approximately a black body with ~ 3000 K color temperature). Thus, since the population of the ground level, 7F_0 , is much larger than the population of all the other levels, all the transitions involving the ground level appear as absorption lines. At room temperature, the population of 7F_2 is negligible and the transition ${}^7F_2 \leftrightarrow {}^5D_0$ is a luminescent one.

The population of the 7F_1 level represents, at room temperature, approximately 15-16% from the entire population. Therefore, it is possible that the luminescence emitted on the ${}^5D_0 \rightarrow {}^7F_1$ transition to be compensated by the reverse (absorption) transition, taking into account the presence of lamp radiation in the respective wavelength domain. The other two transitions involving 7F_1 (${}^7F_1 \leftrightarrow {}^5D_1$ and ${}^7F_1 \leftrightarrow {}^5D_3$) are seen in absorption due to the very low populations of 5D_1 and 5D_3 levels in the given pump conditions (the lamp intensity in UV and blue-green domains is rather low) and due to reduced quantum efficiencies. The same situation (absence of the ${}^7F_1 \leftrightarrow {}^5D_0$ transition) is observed in the spectrum of the Eu- YVO_4 powder (Fig. 5).

From the diffuse reflectance spectra (Fig. 5) we can estimate a measure of the quantum yield as the ratio between the area of the luminescence lines (transition ${}^5D_0 \rightarrow {}^7F_2$) and the area of the absorption Eu^{3+} lines. The spectral distribution of the exciting 'white' light was approximated with the spectral distribution of the 3000 K black body radiation. The total quantity of the absorbed light is proportional with the integral of the absorption spectrum (obtained from the diffuse reflectance spectrum after the extraction of the base line) multiplied with the

spectral distribution of the black body radiation. It results that the efficiency of the Eu-doped LGX crystal powders, calculated in this way, represents approximately 60% from the efficiency of the Eu-YVO₄ powder annealed at 800 °C. We note that the area of the $^5D_0 \rightarrow ^7F_2$ transition for Eu(5%)-YVO₄ powder is more than two times higher than for the Eu(5%)-LGS powder, but the area of the absorption lines is also larger for vanadate (approximately 1.4 times).

A more covalent Eu³⁺ - O²⁻ bond for Eu-doped LGT and LGN would imply a lower energy position of the charge-transfer band (CTB). In [6], we observed that the CTB for Eu:LGX crystals peaks at approximately at the same energy (~300 nm), but its exact position and intensity could be masked by the absorption of the color centers present in LGX crystals.

The influence of the CTB on the luminescence of levels 5D_2 and 5D_3 in Eu:LGN can be seen in Fig. 5 (practically, the same results were obtained for LGT and LGS). The spectra are both normalized to the intensity of the $^5D_0 \rightarrow ^7F_2$ transition for a better visualization. When the sample is pumped on the transition $^5D_0 \rightarrow ^5L_6$, besides the emission lines originating on 5D_0 and 5D_1 , the emission lines of levels 5D_2 and 5D_3 are also visible in the spectrum.

When the sample is pumped in the charge transfer band, the lines originating on 5D_2 and 5D_3 are no longer visible. The emission lines of 5D_0 and 5D_1 also decrease in intensity. A quasi-similar situation was observed for Eu₂(WO₄)₃ where the

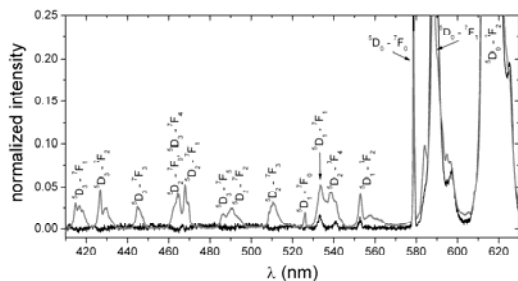


Fig. 5. Emission spectra of Eu³⁺:LGN pumped in the charge-transfer band (thin black line) and by the f-f transition $^7F_0 \rightarrow ^5L_6$ (thick gray line). The spectra are both normalized to the intensity of the $^5D_0 \rightarrow ^7F_2$ transition for a better visualization.

CTB O²⁻ - W⁶⁺ was situated at 260 nm while the CTB O²⁻ - Eu³⁺ at 310 nm [21]. For pumping at 260 nm or at 310 nm the luminescence lines originating in 5D_1 , 5D_2 and 5D_3 are not observed while for pumping at 393 nm ($^7F_0 \rightarrow ^5L_6$) these luminescence lines are visible. These phenomena, also observed in other Eu-doped media, can be due to other de-excitation pathways of the charge-transfer state created by its cross-overs with the 5D_i and 7F_j states [21-25].

4. Conclusions

The radiative lifetime of 5D_0 level was obtained from the area of the luminescence spectrum calibrated with the probability of the magnetic-dipole transition $^5D_0 \rightarrow ^7F_1$.

The obtained values of the quantum efficiency of 5D_0 level were 75% for Eu:LGN, 71% for Eu:LGT and 63% for Eu:LGS. Their subunitary values could be related to transfer to random impurities.

The diffuse reflectance spectra of Eu:LGX powders were obtained with white light excitation. The reflectance curves are tilted towards short wavelength domain, due to the color centers appearing as a result of the thermal treatment in air. Since in these reflectance spectra both absorption and emission lines of Eu³⁺ are simultaneously measured, we propose to use the ratio between the areas of emission and absorption lines as a measure of the relative quantum yield. Compared with Eu:YVO₄ (synthesized by us), the relative quantum yield (for white light excitation) of Eu:LGX crystals represents approximately 60% from the quantum yield of Eu:YVO₄ powder.

When pumped in CTB, its low energy position quenches the luminescence of 5D_3 and 5D_2 levels and reduces the luminescence intensity of 5D_1 other de-excitation pathways of the charge-transfer state created by its cross-overs with the 5D_i and 7F_j states.

Acknowledgements

This work was supported by the National Council of the Scientific Research in Universities (CNCSIS) in the frame of the Project (IDEI) ID 812.

References

- [1] B. V. Mill, A. V. Butashin, G. G. Kodzhabagian, E. L. Belokoneva, N. V. Belov, Doklady Akademii Nauk SSSR **264**, 1385 (1982).
- [2] V. I. Chani, K. Shimamura, Y. M. Yu, T. Fukuda, Mat. Sci. Eng. R **20**, 281 (1997).
- [3] V. N. Molchanov, B. A. Maksimov, A. F. Kondakov, T. S. Chernaya, Yu. V. Pisarevsky, V. I. Simonov, JETP Lett. **74**, 222 (2001).
- [4] S. Georgescu, O. Toma, A. M. Chinie, L. Gheorghe, A. Achim, A. S. Stefan, Optical Materials **30**, 1007 (2008).
- [5] S. Georgescu, O. Toma, A. M. Chinie, L. Gheorghe, A. Achim, A. S. Stefan, J. Lumin. **128**, 741 (2008).
- [6] S. Georgescu, A. M. Voiculescu, O. Toma, C. Tiseanu, L. Gheorghe, A. Achim, C. Matei, Optoelectron. Adv. Mater. – Rapid Commun. **3**, 1379 (2009).
- [7] S. Georgescu, E. Cotoi, A. M. Voiculescu, O. Toma, C. Matei, Romanian J. Phys. **55**, 750 (2010).
- [8] C. Görller-Walrand, L. Fluyt, A. Ceulemans, W. T. Carnall, J. Chem. Phys. **95**, 3099 (1991).
- [9] R. Reisfeld, E. Zigansky, M. Gaft, Mol. Phys. **102**, 1319 (2004).
- [10] M. J. Weber, Phys. Rev. **157**, 262 (1967).
- [11] M. H. V. Werts, R. T. F. Jukes, J. W. Verhoeven, Phys. Chem. Chem. Phys. **4**, 1542 (2002).
- [12] J. Stadel, L. Bohatý, M. Hengst, R. B. Heimann, Crys. Res. Technol. **37**, 1113 (2002).

- [13] T. Taishi, T. Hayashi, N. Bamba, Y. Ohno, I. Yonenaga, K. Hoshikawa, *Physica B* **401–402**, 437 (2007).
- [14] T. Taishi, T. Hayashi, T. Fukami, K. Hoshikawa, I. Yonenaga, *J. Crystal Growth* **304**, 4 (2007).
- [15] G. M. Kuz'micheva, E. N. Domoroschina, V. B. Rybakov, A. B. Dubovsky, E. A. Tyunina, *J. Crystal Growth* **275**, e715 (2005).
- [16] G. M. Kuz'micheva, O. Zaharko, E. A. Tyunina, V. B. Rybakov, I. A. Kaurova, E. N. Domoroshchina, A. B. Dubovsky, *Crystallography Reports* **54**, 279 (2009).
- [17] S. Georgescu, E. Cotoi, A. M. Voiculescu, O. Toma, C. Matei, *Romanian J. Phys.*, **55**, 750 (2010).
- [18] R. C. Ropp, *J. Electrochem. Soc.* **115**, 940 (1968).
- [19] Y. Nobe, H. Takashima, T. Katsumata, *Opt. Lett.*, **19**, 1216 (1994).
- [20] N. Y. Garces, K. T. Stevens, G. K. Foundos, L. E. Halliburton, *J. Phys. Condens. Matter* **16**, 7095 (2004).
- [21] C. Kodaira, H. F. Brito, O. L. Malta, O. A. Serra, *J. Lumin.* **101**, 11 (2003).
- [22] C. W. Struck, W. H. Fonger, *J. Lumin.* **1-2**, 456 (1970).
- [23] G. Blasse, A. Bril, J. A. de Poorter, *J. Chem. Phys.* **53**, 4450 (1970).
- [24] M. D. Chambers, P. A. Rousseve, D. R. Clarke, *J. Lumin.* **129**, 263 (2009).
- [25] Y.-C. Chang, C.-H. Liang, S.-A. Yan, Y.-S. Chang, *J. Phys. Chem. C* **114**, 3645 (2010).

*Corresponding author: serban.georgescu@inflpr.ro